Rasip1-Mediated Rho GTPase Signaling Regulates Blood Vessel Tubulogenesis via Nonmuscle Myosin II

David M. Barry, Yeon Koo, Pieter R. Norden, Lyndsay A. Wylie, Ke Xu, Chonlarat Wichaidit, D. Berfin Azizoglu, Yi Zheng, Melanie H. Cobb, George E. Davis, Ondine Cleaver

Rationale: **Vascular tubulogenesis is essential to cardiovascular development. Within initial vascular cords of endothelial cells, apical membranes are established and become cleared of cell–cell junctions, thereby allowing continuous central lumens to open. Rasip1 (Ras-interacting protein 1) is required for apical junction clearance, as well as for regulation of Rho GTPase (enzyme that hydrolyzes GTP) activity. However, it remains unknown how activities of different Rho GTPases are coordinated by Rasip1 to direct tubulogenesis.**

Objective: **The aim of this study is to determine the mechanisms downstream of Rasip1 that drive vascular tubulogenesis.**

Methods and Results: **Using conditional mouse mutant models and pharmacological approaches, we dissect GTPase pathways downstream of Rasip1. We show that clearance of endothelial cell apical junctions during vascular tubulogenesis depends on Rasip1, as well as the GTPase Cdc42 (cell division control protein 42 homolog) and the kinase Pak4 (serine/threonine-protein kinase 4). Genetic deletion of Rasip1 or Cdc42, or inhibition of Pak4, all blocks endothelial cell tubulogenesis. By contrast, inactivation of RhoA (Ras homologue gene family member A) signaling leads to vessel overexpansion, implicating actomyosin contractility in control of lumen diameter. Interestingly, blocking activity of NMII (nonmuscle myosin II) either before, or after, lumen morphogenesis results in dramatically different tubulogenesis phenotypes, suggesting time-dependent roles.**

Conclusions: **Rasip1 controls different pools of GTPases, which in turn regulate different pools of NMII to coordinate junction clearance (remodeling) and actomyosin contractility during vascular tubulogenesis. Rasip1 promotes activity of Cdc42 to activate Pak4, which in turn activates NMII, clearing apical junctions. Once lumens open, Rasip1 suppresses actomyosin contractility via inhibition of RhoA by Arhgap29, allowing controlled expansion of vessel lumens during embryonic growth. These findings elucidate the stepwise processes regulated by Rasip1 through downstream Rho GTPases and NMII. (*Circ Res*. 2016;119:810-826. DOI: 10.1161/CIRCRESAHA.116.309094.)**

Key Words: actin cytoskeleton ■ endothelial cells ■ morphogenesis ■ myosin type II ■ Ras homologue gene family member A GTP-binding protein ■ Ras interacting protein 1 ■ tubulogenesis

Blood vessels consist of endothelial cells (ECs), connected at their lateral edges by tight and adherens junctions. When endothelial progenitors, or angioblasts, coalesce into primitive cords, they change shape and reorganize their junctions to open, blood-carrying lumens. The formation of vascular lumens is referred to as tubulogenesis and is essential to the passage of blood and serum. Because this process is essential to the viability of all tissues within vertebrate organisms, understanding how blood vessels develop lumens is critical to the study of embryonic development and disease.

A molecular theme underlying both epithelial and endothelial tubulogenesis is signaling by the Rho family of small GTPases (enzyme that hydrolyzes GTP).[1,2] The most highly characterized members of this family include RhoA (Ras homologue gene family member A), Cdc42 (cell division control protein 42 homolog), and Rac1 (Ras-related C3 botulinum substrate 1).[3] Previous studies using cultured ECs have shown that Cdc42 and Rac1 signaling are necessary to stimulate vascular lumen formation, whereas RhoA mediates vessel collapse and regression.[4] During EC tubulogenesis, Rho GTPase activity is regulated by several proteins, including Rasip1 (Ras-interacting protein 1).[5] Rasip1 interacts with an array of GTPases including Ras and Rap1 (Ras-related protein), promoting activity of Cdc42 and Rac1,

Original received May 15, 2016; revision received July 29, 2016; accepted August 2, 2016. In June 2016, the average time from submission to first decision for all original research papers submitted to *Circulation Research* was 13.08 days.

From the Department of Molecular Biology and Center for Regenerative Science and Medicine (D.M.B., Y.K., K.X., D.B.A., O.C.) and Department of Pharmacology (C.W., M.H.C.), University of Texas Southwestern Medical Center, Dallas; Department of Medical Pharmacology and Physiology, University of Missouri, Columbia (P.R.N., G.E.D.); Department of Biology, University of North Carolina, Chapel Hill (L.A.W.); and Division of Experimental Hematology and Cancer Biology, Children's Hospital Research Foundation, University of Cincinnati, OH (Y.Z.).

The online-only Data Supplement is available with this article at http://circres.ahajournals.org/lookup/suppl/doi:10.1161/CIRCRESAHA.116.309094/-/DC1.

Correspondence to Ondine Cleaver, PhD, Department of Molecular Biology, University of Texas Southwestern Medical Center, 5323 Harry Hines Blvd, NA8.300, Dallas, TX 75390. E-mail ondine.cleaver@utsouthwestern.edu

Nonstandard Abbreviations and Acronyms

AJ	adherens junction
CAG	chicken beta actin promoter/enhancer coupled with cytomegalovirus enhancer
Cdc42	cell division control protein 42 homolog
EC	endothelial cell
eGFP	enhanced green fluorescent protein
F-actin	filamentous actin
NMII	nonmuscle myosin II (here, NMII-A or NMHCIIA, also myh9; NMII-B, alsomyh10)
MS1	Mile Sven 1 endothelial line
Pak4	serine/threonine-protein kinase 4
pMLC	phosphorylated myosin light chain
Rab	Ras-related protein (here, Rab5; Rab7; Rab11)
Rac1	Ras-related C3 botulinum substrate 1
Rap1	Ras-related protein
Rasip1	Ras-interacting protein 1
RhoA	Ras homologue gene family member A
ROCK	Rho-associated protein kinase
Tie2	angiopoietin receptor 2
WEC	whole embryo culture

whereas inhibiting RhoA activity.[5–9] Rasip1 and its binding partner, the GTPase-activating protein Arhgap29, inhibit RhoA, which in turn blocks Rho associated kinase (ROCK) signaling.[5,9] RhoA and ROCK normally activate nonmuscle myosin II (NMII) via phosphorylation of its regulatory light chain (phospho myosin light chain [pMLC]). NMII, in turn, controls filamentous actin (F-actin) crosslinking and contractility to regulate cell shape, adhesion, and migration.[10] Previously, Rasip1 was shown to control F-actin contractility, EC–ECM (extracellular matrix) adhesion maturation, and EC–EC adhesion polarity to mediate EC tubulogenesis through modulation of GTPase signaling.[5,11,12] However, how GTPase signaling is coordinated to influence these distinct cellular events remains unknown.

In this study, we uncover that blood vessel tubulogenesis requires 2 Rasip1-governed, spatiotemporally distinct GTPase signaling events that converge onto 1 molecular effector, NMIIA. We show that initial lumen formation depends on angioblast polarization and cell–cell adhesion remodeling. The clearance of cell–cell adhesions from EC preapical membranes requires NMII-dependent actomyosin activity. This activity, in turn, is controlled by Cdc42/Rac1 via regulation of Pak4 (serine/threonine-protein kinase 4), signaling proteins downstream of Rasip1. Inhibition of this pathway results in ectopic apical junctions and blocks tubulogenesis. Once lumens open and the heart starts to beat, nascent vessels experience hemodynamic pressure because of blood flow. We show that restraint of lumen expansion occurs through membrane tension provided by NMII-mediated contractility. This NMII activity is held in check through RhoA suppression by Rasip1-Arhgap29, allowing vessels to expand over developmental time. Inhibition of Rasip1 or Arhgap29 results in narrow lumens, whereas inhibition of RhoA, ROCK, or NMII leads to lumen dilation. We demonstrate that the balance and different timing of NMII activation through Cdc42/Pak versus RhoA/ROCK is critical for blood vessel lumen opening and expansion. This study reveals a reiterative process where GTPases control lumen morphogenesis via differential regulation of NMII activation.

Methods

Mouse and Embryo Handling

All animal husbandry was performed in accordance with protocols approved by the UT Southwestern Medical Center Institutional Animal Care and Use Committee. Embryos were dissected and fixed in 4% paraformaldehyde/PBS for 40 minutes at 4°C and then dehydrated to 75% ethanol for storage at −20°C.

Inducible Deletion of Rho GTPases in Mice

To induce deletion of Cdc42, Rac1, or RhoA using CAG-CreERT2 (tamoxifen-inducible Cre-mediated recombination system driven by the chicken beta actin promoter/enhancer coupled with the cytomegalovirus [CMV] immediate-early enhancer), mothers were gavaged with tamoxifen (3-mg tamoxifen/40-g mouse) at noon during stages E6.5 and E7.5, 36 hours and 12 hours before dissection, respectively. Embryos were dissected at midnight at stage E8.0 (n≥3 for each line).

Whole-Mount Immunofluorescence in Embryos

Whole-mount staining was performed as previously described.[33]

Whole-Mount Immunocytochemistry

Platelet endothelial cell adhesion molecule 1 and platelet endothelial cell adhesion molecule 1/endomucin costain (PE) was performed as previously described.[33]

Immunofluorescence Staining of Embryonic Tissues

Whole-mount staining was performed as previously described.[23] Tyramide signal amplification immunofluorescent staining (PerkinElmer; individual fluorescein tyramide reagent pack, cat# SAT701) was used to stain pMLC.

Immunofluorescence Staining of Cultured ECs

Immunofluorescence staining of Mile Sven 1 endothelial line (MS1) cells was performed as previously described.[23] Staining of human umbilical vein endothelial cells (HUVEC) in 3-dimensional (3D) collagen matrices was performed as previously described.[34]

Hematoxylin and Eosin Staining

Hematoxylin and eosin staining was performed as previously described.[33]

LacZ Staining

Embryos were fixed using glutaraldehyde for 15 minutes, rinsed in PBS, and stained for β-galactosidase overnight (overnight) as previously described.[35] Images were taken with a NeoLumar stereomicroscope (Zeiss) using a DP-70 camera (Olympus).

In Situ Hybridization

In situ hybridization staining on sections and whole mount were performed as previously described.[36] An Arhgap29 3′ coding region fragment (1.2 kb) and a Plexin D1 clone (MMM1013-66046 Open Biosystems) were used to generate Dig-labeled RNA probes.

Small Interfering RNA Transfection and Recombinant Protein Expression

siGENOME small interfering RNAs obtained from GE Dharmacon were transfected into cultured MS1 or HUVEC using standard protocols for transfection and Western blot analysis, as previously described (antibodies used for Western blots are detailed in Online Table S1, and small interfering RNA sequences are detailed in Online Table S2).[37] Transfection of plasmids expressing Rasip1-GFP and GFP was performed 24 hours after small interfering RNA transfection.

Plasmid DNA (1 μg) was transfected onto cells cultured on a 12-mm cover slip using 1-μg Lipofectin (Invitrogen) dissolved in 300-μL Optimem. Cells were fixed and stained 24 hours after transfection.

Transmission Electron Microscopy

Transmission electron microscopy was performed by UTSW Electron Microscopy Core Facility as per their standard protocols.

In Vitro Lumen Formation Assay

HUVEC lumen and tube formation in 3D collagen matrices were performed as previously described.[37]

Whole Embryo Culture

Whole embryo culture protocol was adapted from Mary Dickinson and James Lauderdale.[38,39] Embryos expressing Flk1-enhanced green fluorescent protein (eGFP) were dissected with their yolk sac intact at E8.0 in DMEM containing 8% FBS and 1% antibiotic antimycotic with HEPES. The embryos were cultured for 3 hours in media containing 50% male rat serum and 50% DMEM with HEPES and antibiotics in a Precision Incubator Unit (B.T.C. Engineering Milton Cambridge England). ROCK inhibitor (Y-27632), Pak4 inhibitor (PF-03758309), Rac1-3 inhibitor (EHT), and the NMII inhibitor (blebbistatin) were all added before culture at 10 μmol/L. After culture, embryos were imaged using a Zeiss AxioObserver epifluorescence microscope then fixed at 4°C with 4% paraformaldehyde/PBS for 40 minutes.

Live Imaging

Embryos expressing Flk1-eGFP were dissected with their yolk sac intact at E8.25 in DMEM containing 8% FBS and 1% antibiotic antimycotic with HEPES. The embryos were plated on glass bottom dishes coated with matrigel in media containing 50% male rat serum and 50% DMEM with HEPES. The embryos were then imaged for 4 hours using a spinning disk confocal.

Cell Spreading Assay

A total of 10000 MS1 cells were seeded into a 96-well plate coated with 50 μL of matrigel per well. After 24 hours of culture, the cells were imaged in bright field. The area that the cells cover was quantified using ImageJ software.

Statistics

All data sets were taken from n≥3 biological replicates, with n≥5 to 10 fields of view analyzed. Data are presented as mean±SEM. All statistical analysis was performed using 2-tailed, unpaired Student *t* test in Graphpad Prism software. *P* values <0.05 were considered statistically significant. See Experimental Methods in the Online Data Supplement for detailed statistical analysis using CellProfiler software.

Results

Blood Vessel Lumens Arise Between ECs After Clearance of Apical Adhesions

To assess morphogenesis of blood vessels, we examined vasculogenesis in Flk1-eGFP mouse embryos. Vasculogenesis first occurs in the aorta and the yolk sac at E8.0 (0–1 somite stage). As previously reported, angioblasts arise as scattered mesodermal progenitors that then assemble to form vascular cords (Figure 1A and 1A′ and 1B and 1B′).[13] Angioblasts differentiate into ECs as they flatten and form a lumen at the cord center (Figure 1A′ and 1A″ and 1B′ and 1B″). This process in the aortae occurs in a progressive, anterior-to-posterior manner along the embryonic axis (Online Figure IA). By contrast, live imaging of yolk sac vessels reveals that tubulogenesis in this vascular bed occurs all at once, after the cord network has formed (Figure 1C and 1C′ and Online Movie I).

To examine cellular events during lumen formation (or lumenogenesis), we analyzed EC junctions in E8.0 cords. Sections were stained for the tight junction adhesion molecule zona occludens 1 (ZO-1) and the apical membrane sialomucin podocalyxin. As angioblasts come into contact, they form adhesions between contacting membranes (Online Figure IB through ID). At this preapical surface, podocalyxin becomes polarized and overlaps with adhesion complex foci marked by ZO-1 (Figure 1D through 1D″). Transmission electron microscopy reveals that adhesion complexes stitch ECs together at loci scattered along the preapical membrane, flanking slit-like small luminal spaces (Figure 1G and 1G′). EC membrane at slits take on a concave appearance (Figure 1G′), consistent with podocalyxin separating opposing membranes via electrostatic repulsion.[14] Soon after initial angioblast adhesion, junctions remodel, disappearing from the cord center while enriching peripherally (Figure 1E through 1E″ and 1H; Online Figure IE through E″). During this process, ECs flatten and appear almond shaped in cross section, opening a single central lumen (Figure 1F through F″ and 1I). En face confocal imaging of adhesions at the cord center reveal tight junctions clustered in ribbons that run longitudinally along preapical membranes (cross-sectional view Figure 1J through 1L; en face view Figure 1J′ through 1L′; Online Figure IG). As lumens open, adhesion ribbons shrink and become restricted to basolateral/peripheral regions of the cord, clearing the apical membrane (Figure 1J′ through 1L′). Overall, apical junctional clearance allows a central lumen to open (Figure 1M).

Failed Lumens in Rasip1 Nulls Exhibit Ectopic Apical Junctions

We previously showed that Rasip1 is essential for vascular tubulogenesis and that vascular endothelial cadherin (VEcad) and ZO-1–rich adhesions are observed at the apical membrane of Rasip1$^{-/-}$ cord ECs.[5,15] In the absence of Rasip1, blood vessels fail to open continuous lumens (Figure 2A and 2A′), as mutant ECs are aberrantly stitched together by ectopic apical adhesions, as shown with a platelet endothelial cell adhesion molecule 1/endomucin costain (both red), which are strikingly rich in F-actin (phalloidin, green; Figure 2B through 2C′). Live imaging of Rasip1$^{-/-}$ yolk sac vessels similarly showed failed lumen formation, as ECs within vascular cords failed to form central lumens (Figure 2D and 2D′; Online Movie II).

To further elucidate mechanisms by which Rasip1 regulates EC lumen formation, we assessed its localization in vivo and in vitro. In aortic ECs, Rasip1 was enriched at cell–cell adhesions, as well as transiently along the apical membrane during initial lumen opening (Figure 2E through 2F″). Similarly, HUVEC transfected with Rasip1–GFP and plated either in monolayer cultures or in 3D collagen matrices show strong transient localization to cell–cell adhesions and to the apical membrane during lumen opening, respectively (Online Figure IF and IH through II″). Both in vivo and in vitro Rasip1 was also found to localize to small round cytoplasmic structures near the apical membrane (Figure 2G through 2G″; Online Figure IH through II″). Previous work suggested that Rasip1 localizes to endomembranes.[7] Therefore, we assessed whether Rasip1 was found

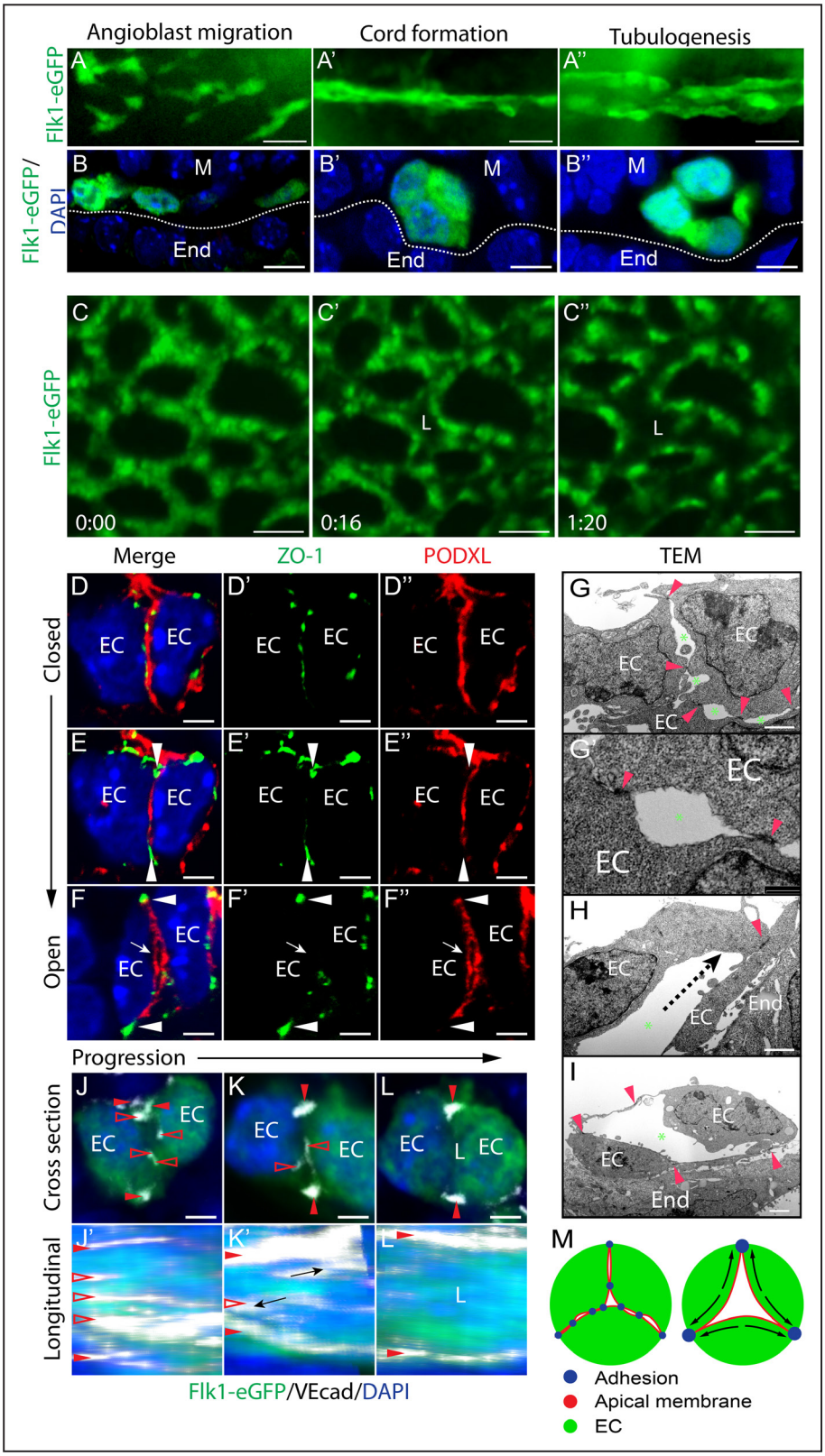

Figure 1. Blood vessel lumens arise between ECs following clearance of preapical adhesions. **A**–**A″**, Flk1-enhanced green fluorescent protein (eGFP) embryos, whole-mount GFP stain (n=3). **B**–**B″**, Cross sections show progression of dorsal aorta cord and lumen formation. **C**–**C″**, Live imaging of Flk1-eGFP yolk sac vasculature. Time in h:min. **D**–**F″**, Progression of tight junctions remodeling away from the apical membrane during lumen formation. Tight junctions, zona occludens 1 (ZO-1), apical membrane, podocalyxin (PODXL; n>10). Arrowhead, adhesions at periphery; arrow, opening lumen. **G**–**I**, transmission electron microscopy (TEM) of aorta cord and opening lumen. Red arrowheads, endothelial cell (EC)–EC adhesion complex; green asterisk, luminal spaces between adhesions; dotted line, direction of adhesion movement. **J**–**L**, Cross sections of EC cords show adhesion remodeling (clearance from preapical membrane). Vascular endothelial cadherin (VEcad), white; Flk1-eGFP, green; open arrowheads, clearing junctions at preapical membrane; closed arrowheads, sustained peripheral junctions. **J′**–**L′**, En face Z-stack confocal image showing apical membrane surface junction ribbons, which are cleared as lumen opens. **M**, Schematic model of lumen formation: adhesions are rearranged to the cord periphery to form a central lumen. Scale bars: **A**–**A″**, 20 μm; **B**–**B″**, 7 μm; **C**–**C″**, 25 μm; **D**–**F″**, 3.5 μm; **G**–**I**, 2 μm; **J**–**L**, 3.5 μm. End indicates endoderm.

on cytoplasmic components such as endosomes. Rasip1 immunostaining was observed to overlap with Rab5 (Ras-related protein) and Rab8, but not with Rab7, suggesting it may be recruited to recycling endosomes (Online Figure IJ through IL). To confirm this, we expressed a constitutively active form of Rab5 (Q79L) that causes early endosomes to fuse and enlarge, and assessed Rasip1 localization. Rasip1 protein was strongly enriched in these structures (Online Figure IM through IM″). Together, these results suggest that

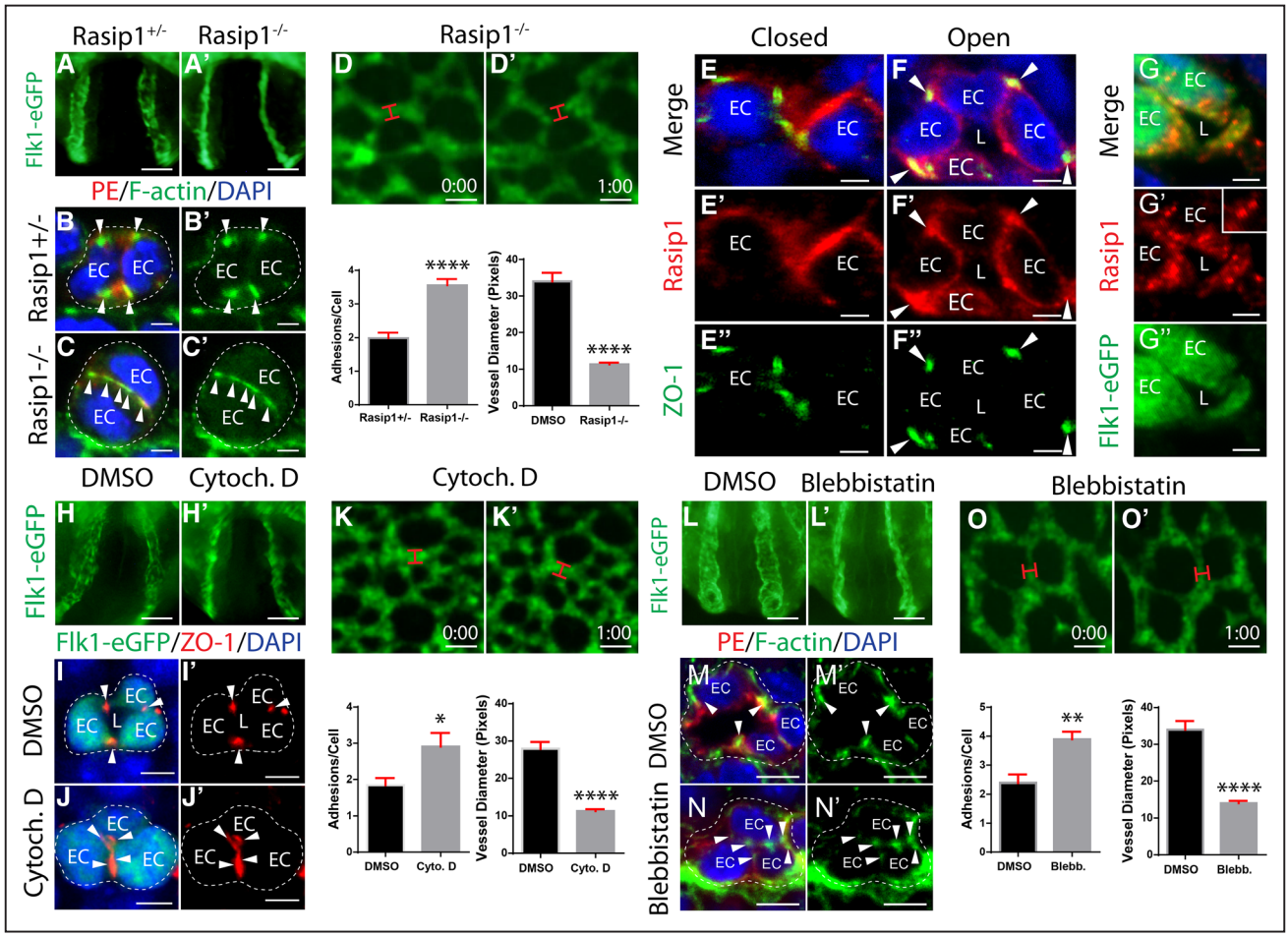

Figure 2. Clearance of endothelial cell (EC) preapical junctions requires Rasip1 and actomyosin contractility. **A** and **A′**, Rasip1 null embryos expressing Flk1-enhanced green fluorescent protein (eGFP) fail to open lumens in the dorsal aorta (n=3 controls, n=3 mutants). **B**–**C′**, Cross sections stained with platelet endothelial cell adhesion molecule 1 and endomucin costain (PE) and F-actin show that Rasip1 mutants fail to remodel adhesions to the periphery of the vascular cord (quantified in graph, n=3 controls, n=3 mutants; 15 fields of view [FOV]). ****P<0.0001. Arrowhead, adhesion. **D** and **D′**, Live imaging of Rasip1$^{-/-}$;Flk1-eGFP embryo yolk sacs (lumen diameter quantified in graph, n=41 control and n=39 mutant). ****P<0.0001. Red bracket, vessel diameter. Time in h:min. **E**–**F″**, Staining of Rasip1 and tight junction marker zona occludens 1 (ZO-1) shows that Rasip1 enriches to adhesions during cord and lumen formation. Arrowheads, adhesions. **G**–**G″**, Staining of Rasip1 localizes at apical membrane after lumen formation. Inset shows endosomal structures. **H** and **H′**, Whole embryo cultures (WECs) treated with cytochalasin D (10 μmol/L) fail to open aortic lumens (n=3 controls, n=3 treated). **I** and **J′**, Cross sections stained for GFP and ZO-1 show that cytochalasin D–treated embryos fail to remodel adhesions to cord periphery (quantified in graph, n=3 controls, n=3 treated; 15 FOV). *P<0.05. **K** and **K′**, Live imaging of cytochalasin D–treated Flk1-eGFP embryos (lumen diameter quantified in graph, n=45 control and n=66 treated). ****P<0.0001. **L** and **L′**, WECs treated with blebbistatin (10 μmol/L) fail to open aortic lumens (n=3 controls, n=3 treated). **M**–**N′**, Cross sections stained with PE and F-actin show that blebbistatin-treated embryos fail to remodel adhesions to cord periphery (quantified in graph, n=3 controls, n=3 treated; 15 FOV). **P<0.01. **O** and **O′**, Live imaging of blebbistatin-treated Flk1-eGFP embryo yolk sacs (lumen diameter quantified in graph, n=41 control and n=20 treated). ****P<0.0001. Scale bars, **A** and **A′** 100 μm; **B**–**C′**, 3.5 μm; **D** and **D′**, 25 μm; **E**–**F″**, 3 μm; **G** and **H″**, 7 μm; **H** and **H′**, 100 μm; **I** and **J′**, 5 μm; **K** and **K′**, 25 μm; **L** and **L′**, 100 μm; **M** and **N′**, 5 μm; **O** and **O′**, 25 μm. EC indicates endothelial cell; and L, lumen.

Rasip1 is recruited to endosomes and EC adhesions and is later recruited to apical membrane.

Clearance of Apical Junctions Requires Actomyosin Contractility

To mechanistically address how Rasip1 might remodel cord EC adhesions away from the apical membrane and restrict them to lateral boundaries, we investigated whether adhesions are normally dismantled and endocytosed, or relocalized. First, whole E8.0 cord stage embryos were cultured (WEC) for 3 hours and treated with Pitstop 2, a drug that inhibits both clathrin-mediated and clathrin-independent endocytosis.[16,17] We found that adhesions were cleared from the apical membrane in both control and Pitstop 2–treated embryos (Online Figure IIA through IIE). Because blocking endocytosis did not perturb adhesion removal from the apical membrane, we hypothesized that adhesions may instead move away from the apical membrane using an actomyosin-dependent force. Consistent with this idea, F-actin and active, serine pMLC were enriched in adhesion complexes, as the adhesions progressively cleared from cord centers (Online Figure IIF through III′).

To determine whether F-actin and myosin are necessary to clear apical adhesions, cord-stage embryos were treated with pharmacological inhibitors. E8.0 Flk1-eGFP WEC was performed for 3 hours in the presence of either cytochalasin

D, which inhibits actin polymerization, or blebbistatin, which blocks NMII ATPase activity. Embryos treated with either inhibitor dramatically failed to clear apical adhesion complexes (Figure 2H and 2H′ and 2L and 2L′). Consequently, cord ECs stayed stitched together and did not form patent lumens (Figure 2I and 2J′ and 2M through 2N′). Live imaging of Flk1-eGFP yolk sacs treated with either drug revealed that continuous vessel lumen formation never took place (Figure 2K and 2K′ and 2O and O′; Online Movies III and IV). These results suggest that F-actin and NMII-mediated F-actin contractility are both essential for remodeling of apical adhesions away from cord centers and are thereby essential for formation of continuous lumens.

Cdc42, But Not RhoA, Signaling Downstream of Rasip1 Is Required for Lumen Formation

We previously showed that Rasip1 regulates the activity of downstream GTPases, Cdc42, Rac1, and RhoA.[5] Indeed, Rasip1 significantly promoted activity of Cdc42 and Rac1 and the downstream kinase Pak4, whereas it suppressed activity of RhoA and its downstream kinase ROCK.[5] Both Cdc42-Pak and RhoA-ROCK signaling are known to play critical roles in organization of the cytoskeleton.[18] Therefore, we asked whether EC lumen formation required either of these 2 signaling cascades, by genetically ablating Cdc42, Rac1, or RhoA in mice, in endothelium before lumen formation. Floxed RhoA, Rac1, or Cdc42 mice (genes flanked by LoxP sequences)[19–22] were crossed to angiopoietin receptor 2 (Tie2)-Cre, which expresses Cre in ECs. In these embryos, although Cre is expressed in angioblasts (Online Figure IIIA and IIIB), protein levels were only depleted before lumen formation in yolk sac vessels, but not in dorsal aortic ECs (Online Figure IIIE through IIIL′). To delete in aortic ECs before lumen formation, the inducible and ubiquitous driver CAG-CreERT2 was used. This allowed early deletion of each gene (after gastrulation, Online Figure IIIC and IIID) and efficient deletion of each protein in aortic cords before lumen formation, with negligible effects on nonendothelial tissues (Online Figure III, induction diagram).

Deletion of Cdc42 in yolk sac vessels using Tie2-Cre, or in aortae using CAG-CreERT2 ($Cdc42^{CAGKO}$), led to a dramatic block in vascular lumen formation, as we previously showed (Figure 3A through 3C′; Online Figure IVA through IVB′).[23] Deletion of Cdc42 blocked lumens in the anterior aortae, as well as inhibited angioblast migration in yolk sac vessels (Figure 3A and 3A′; Online Figure IVA and IVA′). In posterior aortic cords, where mesoderm is still differentiating into angioblasts, loss of Cdc42 impaired migration (Online Figure IVC through IVD′). Similar to $Rasip1^{-/-}$ embryos, ectopic EC apical cell–cell junctions were observed in $Cdc42^{CAGKO}$ cords (Figure 3B through 3C′; Online Figure IVE through IVH′). Live imaging of yolk sac vessels showed that Cdc42-deleted ECs largely fail to form vascular cords, and ECs that do form cords fail to develop lumens (Figure 3D and 3D′; Online Movie V). Cdc42-depleted yolk sac ECs displayed a slight decrease in proliferation (7.2% less) and no change in apoptosis (Online Figure IVI through IVT).

To assess whether the Cdc42-activated kinase Pak4 is necessary for lumen formation downstream of Rasip1 and Cdc42, WEC was performed in the presence of an inhibitor that preferentially blocks Pak4 activity (PF-03758309) for 3 hours. Treatment with the inhibitor blocked lumen formation and apical adhesion remodeling, phenocopying Rasip1 null dorsal aortae (Figure 3E through 3G′). Live imaging of embryos treated with the Pak4 inhibitor showed that vascular cords failed to open any lumens (Figure 3H through 3H′; Online Movie VI). These results suggest that the loss of the Cdc42-Pak4 signaling pathway activity contributes to the failed lumen formation phenotype observed in $Rasip1^{-/-}$ embryos.

In striking contrast, deletion of RhoA or Rac1 using Tie2-Cre or CAG-CreERT2 had no effect on vessel lumen formation (Figure 3I through 3K′; Online Figure V). Although initial lumens formed normally, deletion of RhoA or Rac1 caused embryonic lethality. RhoA mutants displayed overall hypoplasia at E9.25 and Rac1 mutants at E11 (Online Figures VA and VA′ and VIA and VIA′). Deletion of RhoA or Rac1 also led to marked yolk sac vascular remodeling defects at E9.5 (Online Figures VB and VB′ and VIB and VIB′). These findings suggest that Cdc42, Rac1, and RhoA are all necessary for embryonic survival and vascular development. However, although Cdc42 specifically drives clearance of apical EC junctions, RhoA and Rac1 are not required for this process.

RhoA–ROCK–NMII Signaling Suppresses Vessel Expansion

Although RhoA was not necessary for lumenogenesis and apical junction clearance, there was a notable difference in vessel diameter of embryos lacking RhoA. RhoA-depleted aortae were on average 8.6× larger, whereas RhoA-depleted yolk sac vessels were 7.2× larger than controls (Figure 3I through 3K′; Online Figure VIC and VID). Live imaging of yolk sac vessels showed that RhoA-depleted ECs develop dramatically larger lumens (Figure 3L and 3L′; Online Movie VII). At the onset of lumen formation, ECs were markedly more flattened and spread out. The average distance between EC nuclei was increased by 56%, revealing that ECs occupied a larger circumferential area (Online Figure VIE). We note that RhoA-deleted vessels also exhibited a 20% increase in pHH3-positive cells with only a slight increase in apoptosis (Online Figure VIG through VIN). This suggests that RhoA normally restricts lumen diameter through cell shape regulation.

Similarly, we assessed whether the RhoA effector ROCK was necessary for lumen formation. WEC was performed in the presence of the ROCK inhibitor Y-27632 for 3 hours. Inhibition of ROCK dramatically enhanced lumen formation and increased the average distance between aorta nuclei by 23%, phenocopying RhoA-deleted aortae (Figure 3M through 3O′; Online Figure VIF). Live imaging of the yolk sac vasculature under the same conditions also showed that ROCK-inhibited ECs rapidly develop much larger lumens (Figure 3P and 3P′; Online Movie VIII). Together, these data suggest that during vasculogenesis, RhoA–ROCK signaling does not regulate apical junction clearance or lumen formation, but instead stimulates EC contractility to restrain EC spreading and therefore vessel dilation.

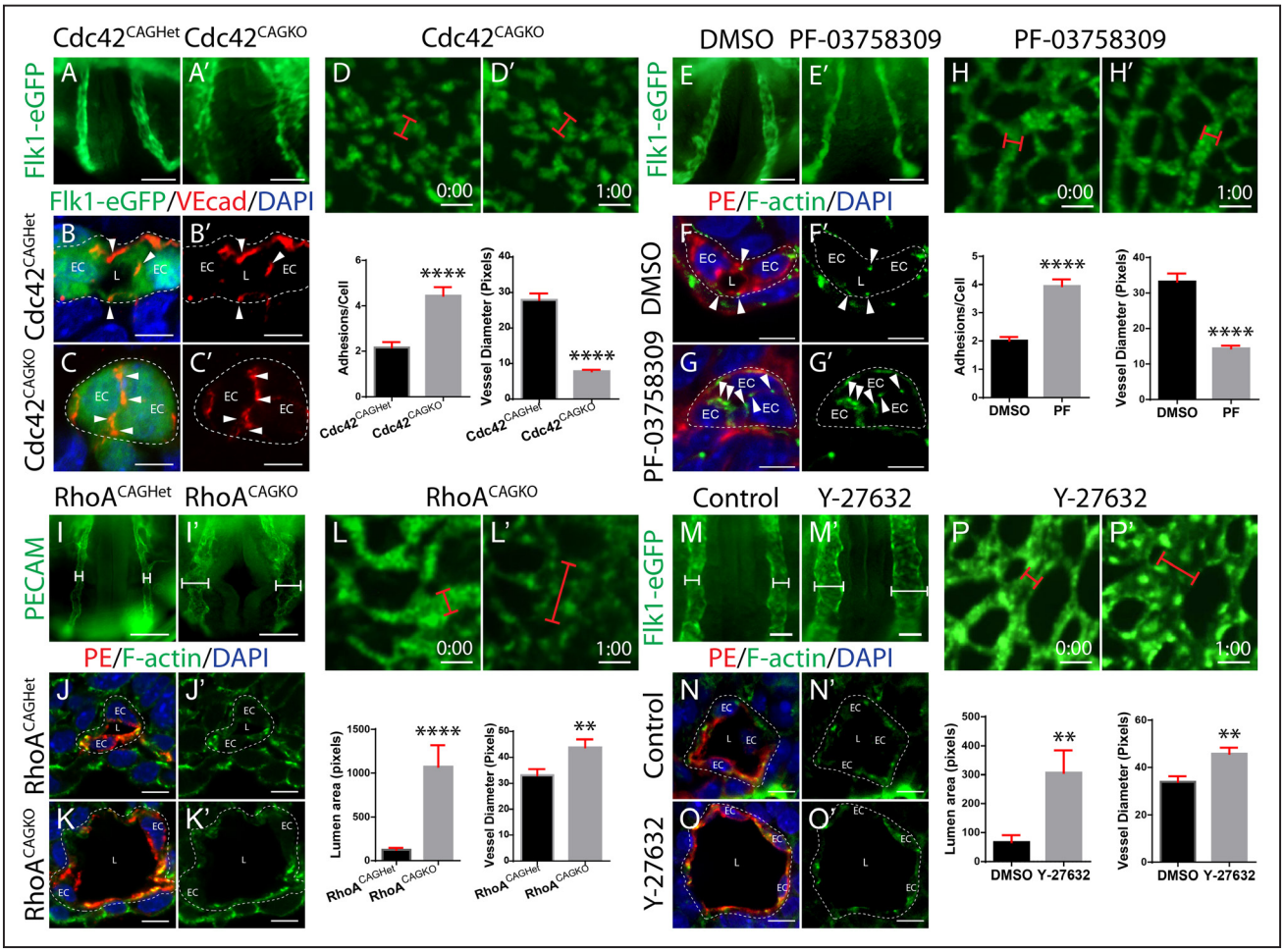

Figure 3. Cdc42, but not RhoA, signaling downstream of Rasip1 is required for lumen formation. **A** and **A′**, Cdc42^{CAGKO} embryos expressing Flk1-enhanced green fluorescent protein (eGFP) fail to open lumens (L) in the dorsal aorta (n>22 controls, n=22 mutants). **B**–**C′**, Cross sections stained for GFP and vascular endothelial cadherin (VEcad) show that Cdc42^{CAGKO} embryos fail to remodel adhesions to the periphery of the vascular cord (quantified in graph, n=3 control, mutant; 15 fields of view [FOV]). ****P<0.0001. Arrowhead, adhesion. **D** and **D′**, Live imaging of Cdc42^{CAGKO} Flk1-eGFP embryo yolk sacs (L diameter quantified in graph, n=45 control and n=38 mutants). ****P<0.0001. Red bracket, vessel diameter. **E** and **E′**, whole embryo cultures (WECs) treated with the serine/threonine-protein kinase 4 (Pak4) inhibitor PF-03758309 (10 μmol/L) fail to open aortic Ls (n=3 controls, n=3 treated). **F**–**G′**, Cross sections stained for endomucin costain (PE) and F-actin show that Pak4-inhibited embryos fail to remodel adhesions to the cord periphery (quantified in graph, n=3 controls, n=3 treated; 15 FOV). ****P<0.0001. **H** and **H′**, Live imaging of Pak4-inhibited Flk1-eGFP embryo yolk sacs (L diameter quantified in **L**, n=40 control and n=33 treated). ****P<0.0001. **I** and **I′**, RhoA^{CAGKO} embryos possess expanded dorsal aortae (n=4 controls, n=4 mutants). **J**–**K′**, Cross sections stained for PE and F-actin show that RhoA^{CAGKO} embryos fail to maintain proper vessel diameter and possess expanded vessels (quantified in graph, n=8 controls, n=8 mutants, 15 FOV). ****P<0.0001. **L** and **L′**, Live imaging of RhoA^{CAGKO} Flk1-eGFP embryo yolk sacs (L diameter quantified in graph, n=40 control and n=36 mutant). **P<0.01. **M** and **M′**, WECs treated with Y-27632 (10 μmol/L) have expanded vessels (n=3 controls, n=3 treated). **N**–**O′**, Cross sections stained for PE and F-actin show that Rho-associated protein kinase (ROCK)–inhibited embryos fail to maintain proper vessel diameter and possess expanded vessels (quantified in graph, n=3 controls, n=3 treated, 15 FOV). **P<0.01. **P** and **P′**, Live imaging of ROCK-inhibited Flk1-eGFP embryo yolk sacs (L diameter quantified in graph, n=41 control and n=49 treated). **P<0.01. Scale bars, **A** and **A′**, 100 μm; **B**–**C′**, 7 μm; **D**–**F′**, 25 μm; **E** and **E′**, 100 μm; **F**–**G′**, 5 μm; **H** and **H′**, 25 μm; **I** and **I′**, 100 μm; **J**–**K′**, 7 μm; **L** and **L′**, 25 μm; **M** and **M′**, 50 μm; **N**–**O′**, 7 μm; and **P** and **P′**, 25 μm. EC indicates endothelial cell.

Arhgap29 and Rasip1 Cooperate to Suppress RhoA-Mediated EC Contractility

Given that an important role ascribed to Rasip1 is suppression of RhoA via Arhgap29, we investigated the role of Arhgap29 during lumenogenesis. Rasip1 and Arhgap29 have both been shown to inhibit RhoA activity in vitro, as knockdown of either protein in cultured ECs causes elevated RhoA activity and failed lumen formation.[5,9,12] To determine whether Arhgap29, or inhibition of RhoA activity, is necessary for blood vessel tubulogenesis, we generated mice with the fourth and fifth exons of Arhgap29 floxed (knockout mouse project repository). Arhgap29 floxed mice were crossed to Sox2-Cre, which expresses Cre in all epiblast cells (embryo proper; Arhgap29^{Sox2KO}). After recombination, Arhgap29 protein is truncated and nonfunctional.

Arhgap29^{Sox2KO} embryos died at midgestation (E9–E10) because of failure of chorioallantoic fusion (Online Figure VIIA through VIIB″). In situ hybridization of Arhgap29 showed enrichment in ECs and the allantois in wild-type embryos (Online Figure VIIC through VIIF′). Arhgap29^{Sox2KO} embryos displayed normal vascular tubulogenesis although lumens became narrower by E8.75–9.0 (Figure 4A through

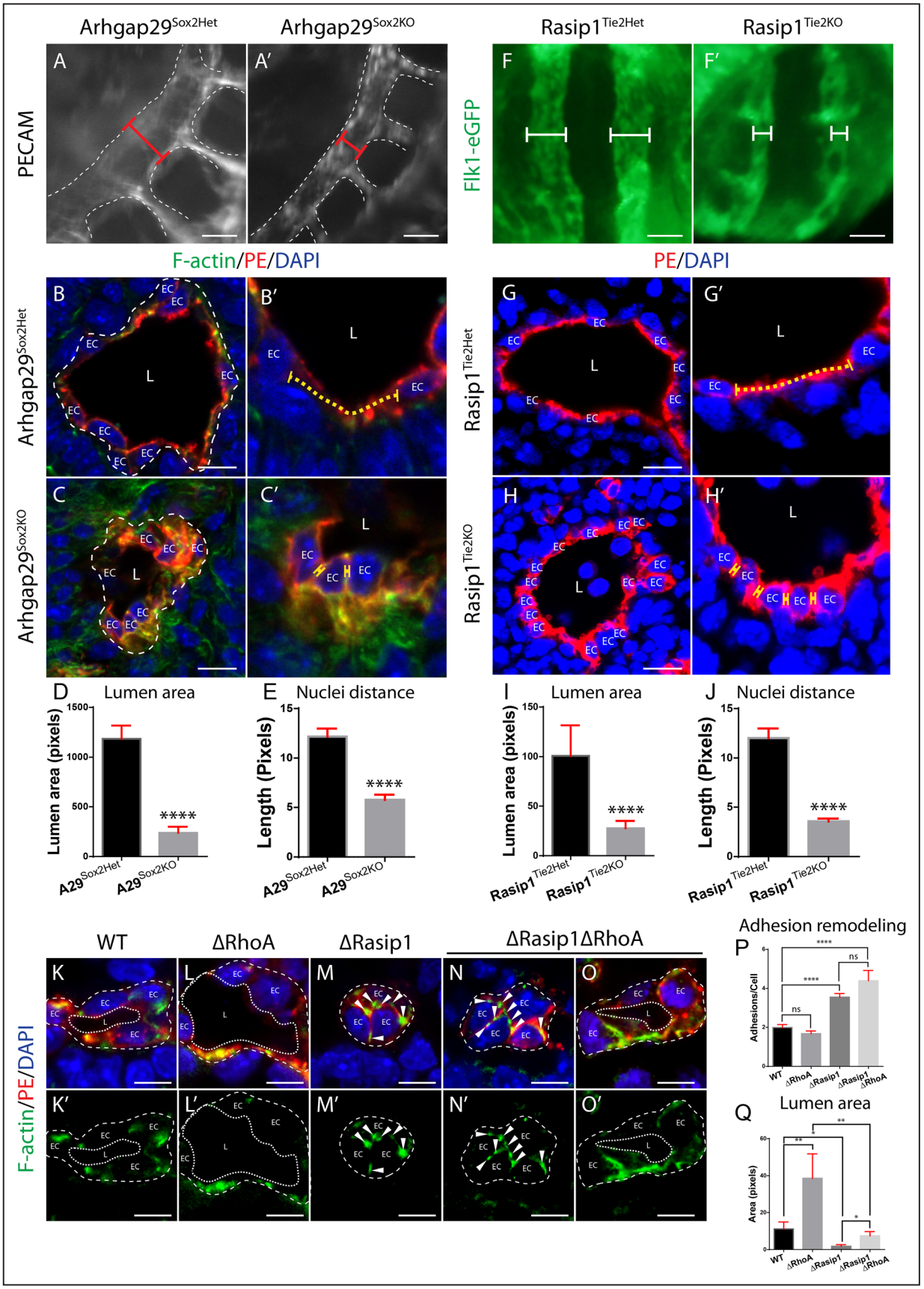

Figure 4. Arhgap29 and Rasip1 (Ras-interacting protein 1) cooperate to suppress Ras **homologue gene family member A (RhoA)–mediated endothelial cell (EC) contractility and lumen expansion. A** and **A′**, Arhgap29^{Sox2KO} embryos stained with platelet endothelial cell adhesion molecule 1 (PECAM) show constricted dorsal aortae (n=3 control and mutant). Red bracket, diameter (*Continued*)

Figure 4 Continued. of vessel. **B–C′**, Cross sections of E8.75 Arhgap29^{Sox2het} and Arhgap29^{Sox2KO} embryos shows vessel constriction after Arhgap29 deletion with smaller vessel lumens and closer adjacent EC nuclei (zoomed-in in **B′** and **C′**, n=3 control and mutant, 15 fields of view [FOV], quantified in **D** and **E**). ****P<0.0001. Yellow dotted line, adjacent nuclei distance. **F** and **F′**, Whole mount images of Flk1-eGFP;Rasip1^{Tie2Het} and Flk1-eGFP;Rasip1^{Tie2KO} embryos show constricted aortae after Rasip1 deletion. White bracket, diameter of vessel. **G–H′**, Cross sections of E8.75 Rasip1^{Tie2Het} and Rasip1^{Tie2KO} embryos shows vessel constriction after Rasip1 deletion with smaller vessel lumens and closer adjacent EC nuclei (zoomed-in in **G′** and **H′**, n= 3 control and mutant, 15 FOV, quantified in **I** and **J**). ****P<0.0001. **K–O′**, Deletion of Rasip1 and RhoA partially rescues lumen expansion but does not rescue adhesion remodeling from the center of vascular cords (n=4 control and mutants, 20 FOV, quantified in **P** and **Q**). Arrowheads, adhesion complexes. L indicates lumen; and ns, not significant. *P<0.05, **P<0.01, ****P<0.0001. Scale bars, **A** and **A′**, 25 μm; **B–C′**, 10 μm; **G–H′**, 10 μm; **K–O′**, 7 μm.

4D). Mutant ECs exhibited normal polarity, as assessed by apical podocalyxin, junctional ZO-1, and basal pPaxillin (Online Figure VIIG through VIIH‴). In contrast to RhoA or ROCK depletion in ECs, which displayed increased cell spreading (nuclei farther apart), the average distance between Arhgap29 null EC nuclei was decreased by 47% relative to controls, suggesting increased internal contractility (Figure 4B′, 4C′, and 4E). To determine whether Rasip1 similarly regulated EC cell shape and contractility, Rasip1$^{f/f}$;Tie2-Cre ECs were assessed. These mice delete Rasip1 several hours after lumen formation.[15] Similar to Arhgap29 mutant vessels, lumens at E8.75 were significantly narrower (Figure 4F through 4I). In cross sections, the average distance between nuclei was decreased by 30%, suggesting increased EC contractility (Figure 4G through 4H′ and 4J). Thus, Arhgap29 likely acts as a Rasip1 effector to suppress RhoA–ROCK–NMII contractility, enabling controlled vessel expansion.

To assess whether Rasip1–Arhgap29 signaling primarily functions to suppress RhoA activity to decrease actomyosin contractility, Rasip1–RhoA double mutants were generated. Control (wild-type) and RhoA null embryos (ΔRhoA) displayed open lumens, with RhoA-null lumens being slightly larger at these early stages (Figure 4K through 4L′). Rasip1 null (ΔRasip1) vascular cords exhibited ectopic apical junctions and discontinuous, interrupted lumens (Figure 4M through 4M′ and 4P). Interestingly, Rasip1–RhoA double mutant (ΔRasip1ΔRhoA) embryos did not rescue adhesion remodeling within vascular cords (Figure 4N through 4N′ and 4P), but did increase lumen area, therefore, partially rescuing lumen formation (Figure 4O and 4O′ and 4Q). This finding suggests that downstream of Rasip1, suppression of RhoA-ROCK activity by Arhgap29, is not necessary for lumenogenesis or apical adhesion remodeling. Instead, the RhoA signaling axis contributes to tension control and internal contractility in ECs, thereby regulating EC spreading and ultimate lumen size.

NMII Acts Downstream of Cdc42–Pak4 to Remodel Apical Adhesions, While Serving as a RhoA–ROCK Effector to Regulate Apical Membrane Tension

Both Cdc42 and RhoA signaling pathways promote NMII activity, yet seem to have opposing influences on lumen formation. We hypothesized that these 2 pathways are spatiotemporally distinct, governing different steps of lumen opening. Specifically, we speculated that Cdc42 activates NMII at cell–cell adhesion complexes to clear them from cord centers, whereas RhoA activates NMII at the apical membrane after lumen formation to provide membrane tension.

To parse out the roles of Cdc42, RhoA and NMII downstream of Rasip1, we examined NMII activity (pMLC Ser19) during adhesion remodeling and lumen expansion. We found that pMLC reduced at cell–cell adhesions in Rasip1 or Cdc42 mutant cords, as well as cords in Pak4-inhibited WECs (Figure 5A through 5F′). In line with its later role, a transient pool of active NMII is observed at the apical membrane (Online Figure VIII through VIIK‴). Deletion of RhoA inhibited apical membrane pMLC, subsequent to lumen opening (Figure 5G through 5H‴). By contrast, deletion of Rasip1 or Arhgap29 led to increased activity of pMLC at the apical membrane (Figure 5I through 5L‴). This suggests that on Rasip1 loss, activated RhoA induces NMII and thus apical membrane contractility. Consistent with this idea, RhoA-deleted ECs displayed a decrease in cell circularity, indicating decreased EC contractility (Figure 5M), whereas Rasip1- and Arhgap29-deleted ECs had increased circularity (Figure 5N through 5O). These data provide evidence that Cdc42-Pak4–dependent NMII activity remodels EC adhesions during lumen opening, whereas RhoA-ROCK–dependent NMII activity promotes apical membrane tension to control lumen diameter.

Cdc42, Pak4, and NMII Pathway Downstream of Rasip1 Supports EC–EC Junctions

To perform spatiotemporal analysis of lumenogenesis, we utilized in vitro systems. To study clearance of adhesions during lumen opening, we modeled adhesion development in vitro. When forming adhesions in vitro, ECs must first find each other and then overlap actin-rich cell processes (also called junctional protrusions[23]) before ultimately establishing mature adhesions. As EC adhesions mature, they become smooth and continuous, and actin filaments remodel from perpendicular to parallel relative to the cell–cell interface. We speculated that the remodeling that takes place in vitro is analogous to adhesion remodeling within vascular cords in vivo. Thus, we depleted with small interfering RNA or inhibited signaling proteins downstream of Rasip1, including Cdc42, Pak4, NMHCIIA, RhoA, or ROCK in MS1 cells, and assessed EC adhesion integrity. Depletion of RhoA or inhibition of ROCK did not affect the integrity of EC adhesions as assessed by VEcad and F-actin staining (Online Figure VIIIA through VIIIE). However, depletion or inhibition of Rasip1, Cdc42, Pak4, or NMHCIIA resulted in dramatically disrupted adhesions (Figure 6A through 6H‴; Online Figure VIIIE). This phenocopied disruption of junctions observed in vivo.[15] Compared with control adhesions with smooth VEcad and F-actin distribution, depleted cells exhibited discontinuous adhesions. Furthermore, F-actin bundles did not align with the cell–cell interface. Thus, adhesion remodeling in vitro recapitulates the in vivo process, where Rasip1-Cdc42-Pak4-NMII signaling regulates vascular adhesion organization, whereas RhoA-ROCK signaling does not. In addition, these

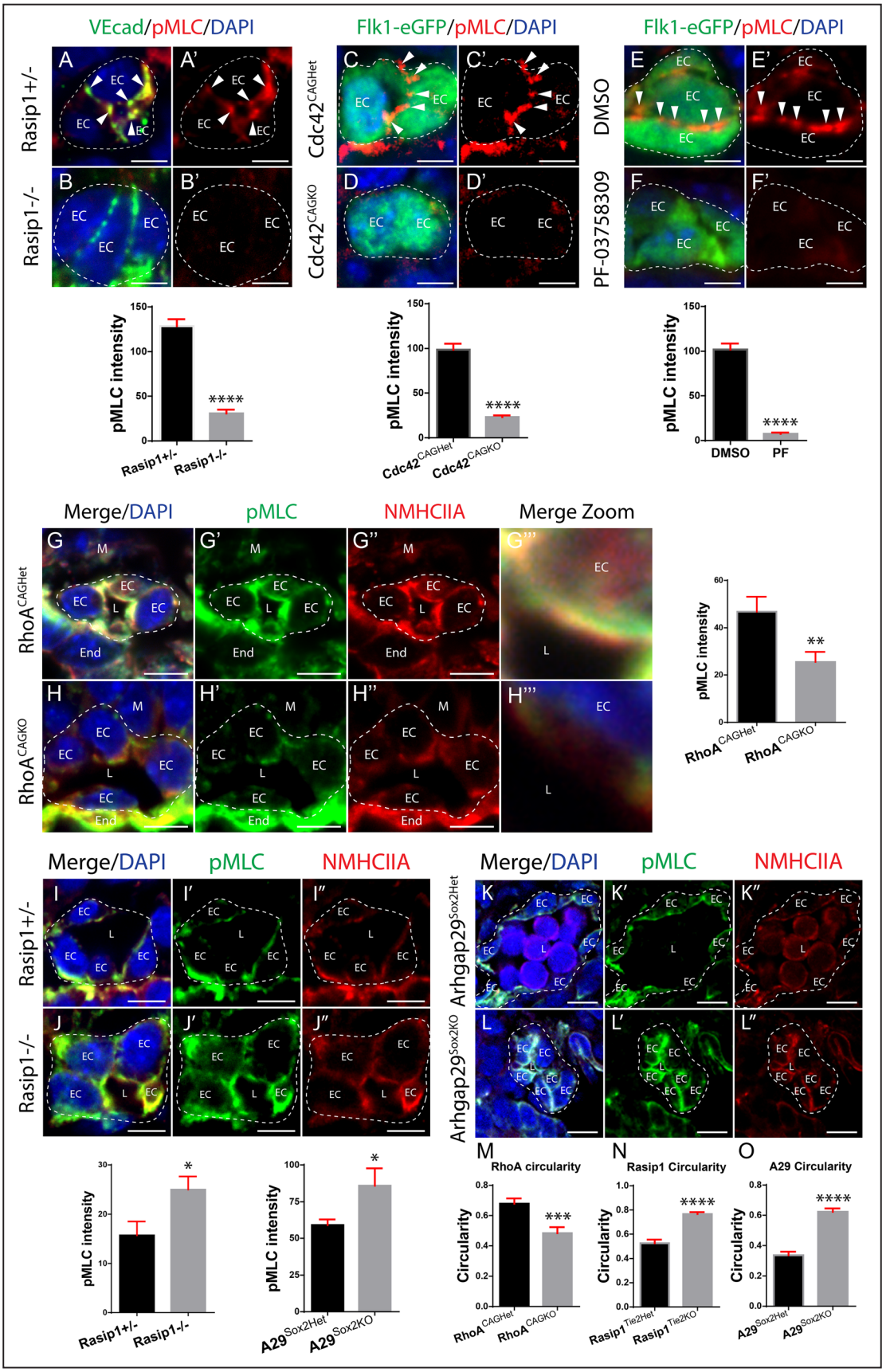

Figure 5. Nonmuscle myosin II (NMII) acts downstream of cell division control protein 42 homolog (Cdc42)-serine/threonine-protein kinase 4 (Pak4) to remodel apical adhesions, while serving as a Ras homologue gene family member A (RhoA)-Rho-associated protein kinase (ROCK) effector to regulate apical membrane tension. A–B′, Staining for vascular endothelial (*Continued*)

Figure 5 Continued. cadherin (VEcad) and phosphorylated myosin light chain (pMLC) on Rasip1$^{+/-}$ (Ras-interacting protein 1) and Rasip1$^{-/-}$ embryos shows that Rasip1 is necessary for NMII activity during vascular cord adhesion remodeling (n= 3 control and mutants/WECs, 15 fields of view [FOV], quantified in graph). ****P<0.0001. Arrowheads, adhesion complex pMLC. **C**–**D′**, Staining of Flk1-eGFP and pMLC on Cdc42^{CAGHet} and Cdc42^{CAGKO} embryos shows that Cdc42 is necessary for NMII activity during cord adhesion remodeling (n=3 control and mutant, 15 FOV, quantified in graph). ****P<0.0001. **E**–**F′**, Staining of Flk1-eGFP and pMLC on DMSO and PF-03758309-treated WECs shows that Pak4 is necessary for pMLC activity during cord adhesion remodeling (n=3 control and treated, 15 FOV, quantified in graph). ****P<0.0001. **G**–**H″**, Staining for NMHCIIA and pMLC on RhoA^{CAGHet} and RhoA^{CAGKO} embryos shows that RhoA is necessary for NMII activity at the apical membrane during lumen formation (n=3 control and mutant, 15 FOV, quantified in graph). **P<0.01. **I**–**J″**, Staining of NMHCIIA and pMLC on Rasip1$^{+/-}$ and Rasip1$^{-/-}$ embryos shows that Rasip1 is necessary to suppress NMII activity at the apical membrane during lumen formation (n=3 control and mutant, 15 FOV, quantified in graph). *P<0.05. **K**–**L″**, Staining of NMHCIIA and pMLC on Arhgap29^{Sox2Het} and Arhgap29^{Sox2KO} embryos shows that Arhgap29 is necessary to suppress NMII activity at the apical membrane during lumen formation (n=3 control and mutant, 15 FOV, quantified in graph). *P<0.05. **M**–**O**, Quantification of EC circularity after deletion of RhoA, Rasip1, or Arhgap29, respectively (n= 3 control and mutants, 15 FOV). ***P<0.001. ****P<0.0001. Scale bars, **A**–**F′**, 5 μm; **G**–**H″**, 7 μm; **I**–**L″**, 10 μm. EC indicates endothelial cell; End, endoderm; L, lumen; and M, mesoderm.

results suggest that this process is regulated by NMII control of F-actin at EC cell–cell adhesions.

To test whether disruption of adhesions by NMII depletion or inhibition correlates with failed lumen formation in vitro, 3D lumen formation assays were performed in the presence of blebbistatin, or siNMHCIIA, siNMHCIIB, or both. Treatment of HUVEC with 10 to 20 μmol/L blebbistatin or siNMHCIIA blocked lumen formation in 3D collagen matrices (Figure 6I and 6J). Reduction of NMHCIIA and NMHCIIB together prevented lumen formation more efficiently than NMHCIIA or NMHCIIB reduction alone (Figure 6K). These results show that NMII is vital for EC tubulogenesis. NMII is regulated by several proteins that are directly controlled by Cdc42, Rac1, and RhoA, including Pak2, Pak4, MRCKβ (myotonic dystrophy kinase–related Cdc42-binding kinase β) and ROCK.[10,23] To determine which proteins control NMII-dependent lumen formation, we depleted each protein in HUVEC and performed 3D lumen formation assays. Only reduction of the Cdc42 effectors Pak2, Pak4, or MRCKβ prevented lumen formation (Figure 6L through 6Q). Thus, both our in vivo and in vitro data suggest that only the Cdc42-NMII pathway, and not the RhoA-ROCK-NMII pathway, regulates NMII-dependent lumen formation.

NMII Temporally Stimulates Lumen Formation and Then Suppresses Cell Spreading and Lumen Expansion via RhoA-ROCK Signaling

Because NMII activity was first identified within cord adhesion complexes in a Cdc42-Pak4–dependent manner and later at the apical membrane in a RhoA-ROCK–dependent manner, we hypothesized that Cdc42-Pak4–dependent NMII activity regulates adhesion remodeling before lumen opening, whereas RhoA-ROCK–dependent NMII activity regulates subsequent apical membrane constriction. To directly test this timing issue in vitro, we inhibited total NMII activity with blebbistatin or RhoA-dependent NMII activity using the ROCK inhibitor Y-27632, either before (0–72 hours) or after (48–72 hours) lumen formation in a 3D lumen formation assay. We reasoned that early blebbistatin-mediated NMII inhibition would block Cdc42-dependent NMII activity in cords, while later ROCK inhibition would block RhoA-dependent NMII activity after lumen opening. We found that the treatment with blebbistatin prevented lumen formation, only when treated at the onset of the assay, but did not affect blood vessel lumen size when treated 48 hours after lumen opening (Figure 7A). By contrast, inhibition of ROCK had no influence on lumen formation, but instead led to larger vessel diameters when treated 48 hours after lumen opening (Figure 7A). These results suggest that NMII temporally and spatially controls different aspects of vasculogenesis, downstream of different GTPases. Activated by Cdc42 and Pak4, NMII controls adhesion organization and lumen formation, whereas downstream of RhoA, NMII controls EC contractility to prevent vessel overexpansion.

To further test whether RhoA, ROCK, or NMII regulate cell shape and spreading in vitro, MS1 cells on Matrigel were treated with siRhoA, siNMHCIIA, or with ROCK or NMII inhibitors. Control MS1 cells formed tight EC aggregates after 24 hours when plated at low confluency. RhoA depletion or ROCK inhibition significantly increased overall cell area (spreading), suggesting that these proteins regulate cell shape through the actomyosin machinery (Figure 7B and 7C and 7E and 7F). By contrast, NMIIA-depleted or NMIIA-inhibited cells failed to aggregate (Figure 7D and 7G). Thus, total NMII (including Cdc42-dependent NMII) is necessary for cell–cell adhesion, whereas a specific NMII pool regulates cell contractility downstream of RhoA-ROCK signaling.

We next asked whether RhoA-ROCK-NMII signaling stimulates EC contractility after lumen formation. MS1 stress fiber development and cell spreading were measured after depletion of RhoA, ROCK, or NMII or constitutively active RhoA(V14) overexpression. Indeed, depletion of RhoA, ROCK, or NMII activity prevented stress fiber formation and caused ECs to dramatically increase in cell area (Figure 7H through 7K). Conversely, overexpression of RhoA(V14) caused ECs to greatly contract and create excess stress fibers (Figure 7L through 7M′). These results suggest that RhoA-ROCK-NMII signaling stimulates EC contractility during blood vessel development.

Finally, to further test whether NMII controls actomyosin contractility and membrane tension after lumen formation, WEC of embryos with open lumens (2–3 somite stage) were treated with blebbistatin for 2 hours. Control embryos developed aortae with a normal diameter, whereas blebbistatin-treated embryos exhibited markedly dilated lumens, resembling ROCK-inhibited embryos (Figure 7N through 7O′). To determine how NMII affects lumen area and EC contractility after lumen formation in real time, live imaging Flk1-eGFP yolk sacs was performed in the presence of

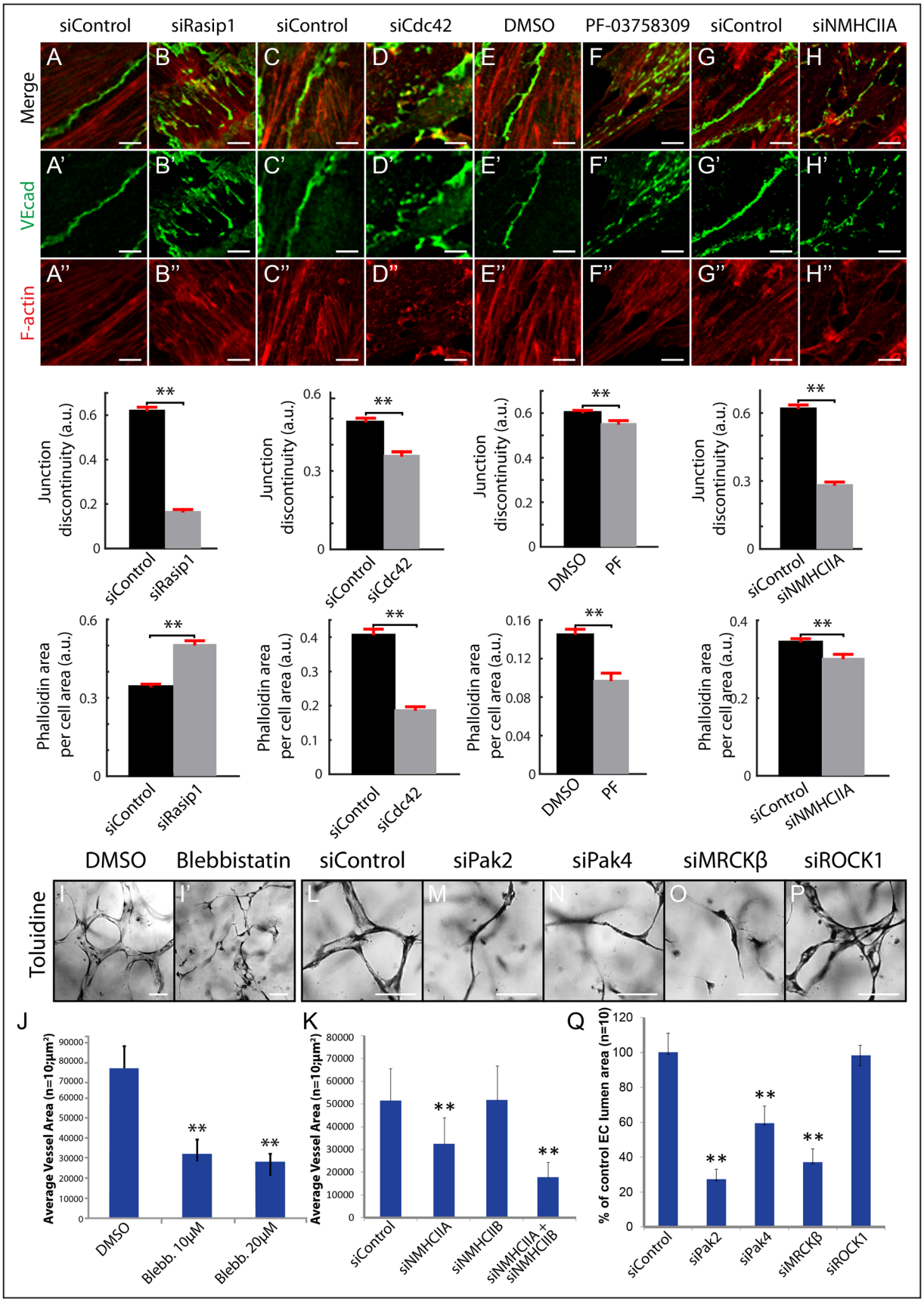

Figure 6. Cell division control protein 42 homolog (Cdc42), serine/threonine-protein kinase 4 (Pak4), and nonmuscle myosin II (NMII) pathway downstream of Rasip1 (Ras-interacting protein 1) supports endothelial cell (EC)–EC junctions and vascular lumenogenesis. A–H″, Staining and quantification of vascular endothelial cadherin (VEcad) continuity and F-actin area at Mile (*Continued*)

Figure 6 Continued. Sven 1 endothelial line (MS1) EC cell–cell junctions after small interfering RNA (siRNA) reduction of Rasip1, Cdc42, or NMHCIIA, or pharmacological inhibition of Pak4 (n=3 control and treated, 15 fields of view [FOV]). ***P*<0.01. **I** and **J**, Inhibition of NMII via 10 or 20 μmol/L blebbistatin treatment prevents EC lumen formation in 3D collagen matrices (quantified in **J**). ***P*<0.01. **K**, Graph showing that reduction of NMHCIIA or NMHCIIA and NMHCIIB combined, but not of NMHCIIB alone, prevents EC lumen formation in 3D collagen matrices. ***P*<0.01. **L–Q**, siRNA reduction of Cdc42 effectors Pak2, Pak4, or myotonic dystrophy kinase–related Cdc42-binding kinase (MRCK) β but not RhoA effector ROCK prevents EC lumen formation in 3D collagen matrices (quantified in **Q**). ***P*<0.01. Scale bars, **A–N″**, 5 μm; and **I–P**, 100 μm.

blebbistatin or the ROCK inhibitor Y-27632. Control vessels maintained a consistent lumen diameter over the course of 40 minutes (Figure 7P through 7P1′ and Online Movie IX). Treatment with blebbistatin caused vessels to expand by 42% (Figure 7Q and 7Q1′; Online Movie X). Treatment of Y-27632 similarly caused vessels to dilate and the vessel area to increase by 37% (Figure 7R and 7R′; Online Movie XII). Close tracking of adjacent ECs showed significant spreading after drug treatment, increasing the space between ECs by 35% after blebbistatin treatment and by 36% after Y-27632 treatment (Figure 7P1 through 7P1′ and 7Q1 and 7Q1′, and 7R1 and 7R1′). These results demonstrate that NMII possesses a RhoA-ROCK–dependent role, separable from its Cdc42-dependent role, whereby it stimulates EC contractility to suppress lumen dilation. Overall, our data suggest a novel mechanism whereby Rasip1 suppresses apical NMII activity to allow lumen expansion over the course of embryonic growth.

Discussion

In this study, we dissect how Rho GTPase signaling pathways coordinate to regulate distinct cellular events driving blood vessel lumen formation during vasculogenesis (Figure 8, model). Angioblasts first form cell–cell adhesions as they assemble into cords, and thereby establish apicobasal polarity. As EC tubulogenesis initiates, cell–cell adhesions anchored by actin are cleared from the preapical membrane and restricted laterally. The EC preapical membrane will remodel over time to become a mature apical surface during the tubulogenic process. Reorganization of adhesions in aortic ECs depends on Rasip1 and Cdc42-Pak4-NMII pathway regulation of actin organization. Shortly thereafter, the heart begins to pump plasma into early vessels, expanding nascent lumens. We show that this expansion is controlled by Rasip1 and by the RhoA-ROCK-NMII pathway. NMII and actin are recruited to the apical membrane, where they restrain membrane expansion and lumen size. However, as vessels must grow, Rasip1 balances membrane tension by inhibition of RhoA via Arhgap29. These mechanisms regulate specific cellular events that drive blood vessel formation and expansion in a tightly regulated manner.

Regulation of Adhesion Organization via Rasip1 and Cdc42-Pak4-NMII

We previously demonstrated that Rasip1 is an essential factor for vascular tubulogenesis. Specifically, we showed that Rasip1 is required for β1-integrin– and β3-integrin–dependent EC–ECM adhesion, as well as remodeling adhesions away from the EC apical membrane within vascular cords. Moreover, we showed that Rasip1 activates Cdc42 and Rac1, which in turn activate the kinase Pak4. Interestingly, Pak4, as well as MLC kinase, is known to control actin contractility by activating NMII, via phosphorylation of MLC. Previous studies identified roles for Cdc42 and NMII in the building of circumferential actin bundles that promote formation of linear and tight adherens junctions.[24] Rasip1 has also been shown to recruit NMIIB to promote EC-cell adhesion.[6] Reduction of Rasip1 caused EC–EC adhesions to become disrupted, nonlinear, and dissociated from actin. These studies suggest that Rasip1-Cdc42-Pak4-NMII signaling promotes adhesion reorganization.

Here, we show that inhibition of Rasip1, Cdc42, Pak4, or NMII suppresses proper adhesion development in vitro. We show that similar mechanisms are at play in vivo, where loss of activity of these components causes failed adhesion redistribution within vascular cords. Whether clearance of junctions in cords (shrinking of junction ribbons) occurs via mechanical sliding along actin tracks to the cord periphery or via actin-based vectorial apical transport of membrane remains unclear. The former is suggested by studies of actomyosin-dependent junction remodeling required in numerous morphogenetic processes, such as during *Drosophila* germband extension.[25,26] Additional studies will be necessary to determine whether Rasip1 directly influences adhesions through scaffolding adhesion complexes or actin crosslinking molecules (such as NMII), or whether Rasip1 regulates adhesion integrity solely through signaling and nonscaffolding mechanisms, such as vesicular transport.

Rasip1 and Arhgap29 Inhibit RhoA-ROCK-NMII Signaling to Allow Lumen Expansion

EC contraction is regulated by actin–myosin contractility, and inhibition of EC contraction leads to cell spreading. The Rap1–Rasip1–Arhgap29 complex has been shown to induce cell spreading by inhibiting RhoA-ROCK-NMII signaling and actin contractility.[5,9,11,12] By suppressing EC contractility, Rasip1 and Arhgap29 may promote cell spreading and allow controlled expansion of vessel lumens, as the embryo grows. Consistent with this idea, deletion of Rasip1 or Arhgap29 after lumen formation causes increased EC contractility and blocks lumen expansion. Conversely, RhoA-ROCK-NMII–dependent actin contractility may normally function to prevent dilation of the lumen by resisting cell spreading. Supporting this, perturbation of RhoA, ROCK, or NMII in vivo after lumen formation leads to dilated vessel lumens. A similar role for the actomyosin contractility machinery in restraint of lumen size has been reported in zebrafish intersomitic vessels, in *Ciona intestinalis* notochord development, and in the developing pancreas.[27–29] In zebrafish, ECs were found to resist plasma membrane deformation (blebbing) via rapid recruitment of myosin and induction of myosin-mediated cortical actin constriction.[27] Thus, we propose that a balance is required, where RhoA-ROCK-NMII signaling stimulates vessel contraction to prevent it from dilating, and

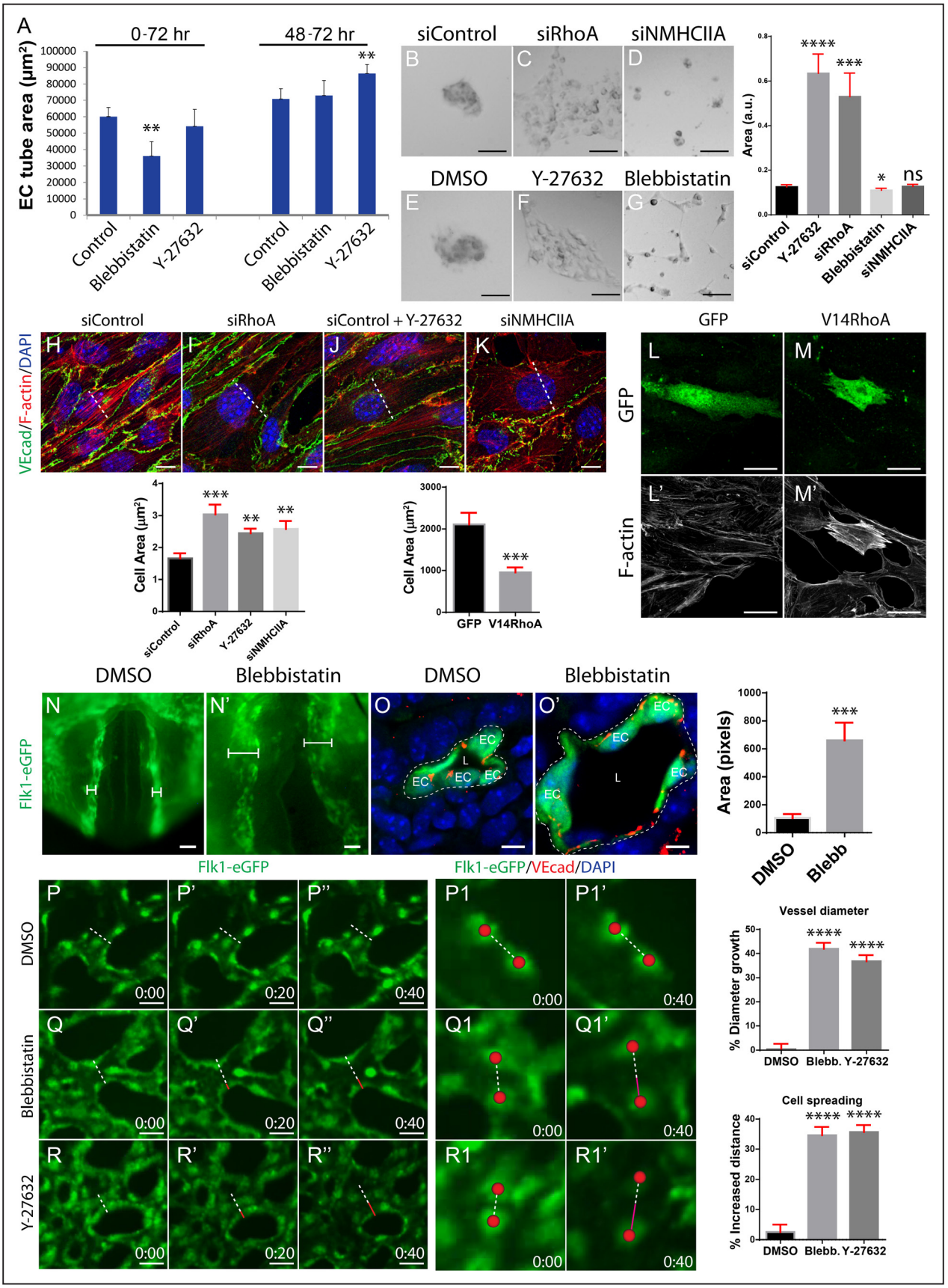

Figure 7. Nonmuscle myosin II (NMII) temporally stimulates lumen formation, then suppresses cell spreading and lumen expansion via Ras homologue gene family member A (RhoA)-Rho-associated protein kinase (ROCK) signaling. A, Graph depicting vessel area in a 3D endothelial cell (EC) lumen formation assay after treatment with blebbistatin or Y-27632 before lumen formation (*Continued*)

Figure 7 Continued. (0–72 h) or after lumen formation (48–72 h). ***P*<0.01. **B–G**, Matrigel cell aggregation assay after small interfering RNA (siRNA) reduction of RhoA or NMHCIIA or treatment with Y-27632 or blebbistatin (n>50 control and treated, 9 fields of view [FOV], quantified in graph). **P*<0.05, ****P*<0.001, *****P*<0.0001. **H–K**, Mile Sven 1 endothelial line (MS1) cells stained for Vascular endothelial cadherin (VEcad) and F-actin to assess stress fiber development and cell spreading after siRNA reduction of RhoA or NMHCIIA or pharmacological inhibition of ROCK (n=3 control and treated, 15 FOV, cell spreading quantified in graph). ***P*<0.01, ****P*<0.001. Dotted line, lowest central diameter. **L–M′**, GFP and F-actin staining after adenoviral infection of GFP or V14RhoA+GFP in MS1 cells to assess cell spreading and actin contractility (n>15 control and treated, 15 FOV, cell spreading quantified in graph). **N** and **N′**, Two-hour whole embryo cultures of Flk1-eGFP embryos treated with blebbistatin after initial lumen formation of the dorsal aorta (n=3 control and treated). Brackets, vessel diameter. **O** and **O′**, Cross sections show that NMII inhibition after initial lumen formation causes vessels to expand (n=3 control and treated, 15 FOV, quantified in graph). ****P*<0.001. **P–R″**, Live imaging of Flk1-eGFP yolk sac vessels treated with either blebbistatin or Y-27632 after lumen formation (n=20 control and treated, change in vessel diameter size quantified in graph). Images are snap shots at 0, 20, and 40 min. *****P*<0.0001. Dotted line, starting vessel diameter; red line, increased length of vessel diameter. **P1–R1′**, Tracking of EC spreading after blebbistatin or Y-27632 treatment for 40 min (quantified in graph). *****P*<0.0001. Red sphere, EC center; dotted line, starting distance between cells; magenta line, increased distance between cells. Scale bars, **B–G**, 50 μm; **H–K**, 10 μm; **L–M′**, 25 μm; **N** and **N′**, 20 μm; **O** and **O′**, 5 μm; and **P–R″**, 25 μm. Ns indicates not significant.

Rasip1-Arhgap29 suppresses RhoA-ROCK-NMII signaling to allow vessel expansion during growth.

Spatiotemporally Distinct Roles of NMII Through Distinct GTPase Activities

Our data support the paradigm that Rasip1 controls different pools of GTPases. These, in turn, regulate different pools of NMII to coordinate actomyosin contractility in distinct cellular processes during vessel tubulogenesis. Because both Cdc42 and RhoA signaling pathways promote NMII activity, yet seem to have opposing influences on lumen formation, we sought to clarify the role of these pathways in forming blood vessels. We hypothesized that during EC lumen formation, RhoA controls the activity of an NMII pool at the apical membrane, whereas Cdc42 controls NMII at cell–cell adhesion complexes. In addition, we predicted that these different functions were likely temporally distinct, given the time course of events during vasculogenesis. This hypothesis finds support in studies that show that the RhoA-ROCK and Cdc42-Pak-MLC kinase pathways act on distinct pools of NMII.[30] In fibroblasts, MLC kinase inhibition blocks MLC phosphorylation at the cell periphery, but not at the cell center, whereas ROCK inhibition blocks MLC phosphorylation in the cell center, but not in the periphery. Similarly, different GTPases control different subcellular processes: RhoA primarily controls stress fiber development, whereas Cdc42 controls cell–cell adhesions, membrane ruffling, and filopodia.[31,32] A recent study by Ando et al[24] showed that RhoA uses NMII to regulate radial stress fiber development into rigid permeable focal AJs, whereas Cdc42 uses NMII to regulate the development of linear stable adhesions with circumferential bundles of actin. Our findings similarly suggest that different NMII pools come into play at different steps of lumen formation. Temporal inhibition of NMII helped us distinguish its different roles at different time points during vascular lumenogenesis and growth. However, studies on in vivo subcellular distribution of these signaling pathways are still needed and will further our understanding of blood vessel development.

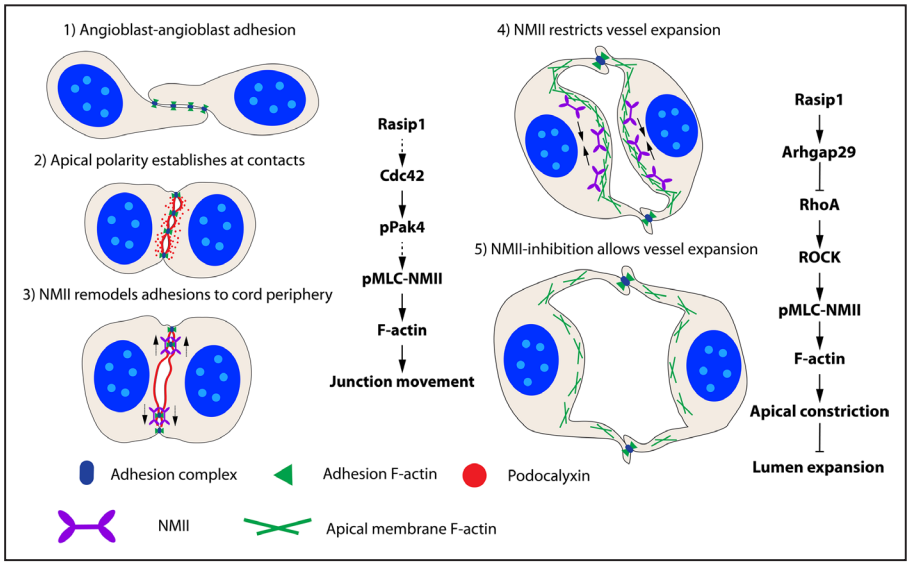

Figure 8. Model of tubulogenesis and vessel expansion during vasculogenesis. (1) Angioblasts develop from mesodermal tissue and form punctae of adhesions with adjacent angioblasts. (2) At the angioblast cell-cell contact, podocalyxin is polarized between the cells, overlapping with the cell adhesion complexes. (3) After activation by Rasip1 (Ras-interacting protein 1) and cell division control protein 42 homolog (Cdc42)-serine/threonine-protein kinase 4 (Pak4) signaling, nonmuscle myosin II (NMII) uses its contractile abilities on F-actin to redistribute adhesion complexes away from the preapical membrane to the cord periphery, exposing a single luminal space. (4) After lumen formation is complete, the lumen opens in a controlled manner. Ras homologue gene family member A (RhoA)-Rho-associated protein kinase (ROCK)–activated NMII suppresses excessive expansion of the lumen by constricting F-actin within endothelial cells and at the apical membrane. (5) As the lumen expands, NMII activity is relaxed by inhibiting RhoA-ROCK-NMII signaling through Rasip1 and Arhgap29.

In conclusion, we find that endothelial lumen formation occurs in a step-wise process that is regulated by Rasip1, Rho family GTPases, and NMII. We show here that an essential step in this process is clearance of adhesions from the apical membrane to allow the formation of a single, continuous lumen. We further demonstrate how blood vessel lumen diameter is tightly regulated, to maintain proper lumen size and integrity. Our study uncovers a coordinated action of Rho GTPases governed by Rasip1 to enable proper vasculogenic tubulogenesis.

Acknowledgments

We thank Janet Rossant for Flk1-eGFP, Thomas Carroll for CAG-CreERT2 and Tom Sato for Tie2-Cre mouse lines, and Neal Alto for the Rab5^{CA} construct. We thank Hiromi Yanagisawa for use of cell culture equipment, the TIG group, and the Carroll, Olson, MacDonald, and Cleaver laboratories for invaluable discussions and assistance. We thank Caitlin Braitsch for critical reading of the article. Most experiments were performed by D.M. Barry, Y. Koo, P.R. Norden, and L.A. Wylie, K. Xu, C. Wichaidit, and D.B. Azizoglu performed supportive experiments. Y. Zheng and M.H. Cobb provided reagents and expertise, and G.E. Davis contributed to underlying ideas and analysis, and contributed 3D in vitro data. All authors read the article critically. O. Cleaver supervised the overall project and contributed to the analysis. D.M. and O. Cleaver wrote the article.

Sources of Funding

This work was supported by National Insritutes of Health R01HL113498 to D.M. Barry, R01HL105606 and R01HL108670 to G.E. Davis, and CPRIT RP110405, 5R01HL113498, R01HL126518, and R01DK079862 to O. Cleaver.

Disclosures

None.

References

1. Iruela-Arispe ML, Davis GE. Cellular and molecular mechanisms of vascular lumen formation. *Dev Cell*. 2009;16:222–231. doi: 10.1016/j.devcel.2009.01.013.
2. Davis GE, Stratman AN, Sacharidou A, Koh W. Molecular basis for endothelial lumen formation and tubulogenesis during vasculogenesis and angiogenic sprouting. *Int Rev Cell Mol Biol*. 2011;288:101–165. doi: 10.1016/B978-0-12-386041-5.00003-0.
3. Etienne-Manneville S, Hall A. Rho GTPases in cell biology. *Nature*. 2002;420:629–635. doi: 10.1038/nature01148.
4. Bayless KJ, Davis GE. The Cdc42 and Rac1 GTPases are required for capillary lumen formation in three-dimensional extracellular matrices. *J Cell Sci*. 2002;115:1123–1136.
5. Xu K, Sacharidou A, Fu S, Chong DC, Skaug B, Chen ZF, Davis GE and Cleaver O. Blood vessel tubulogenesis requires Rasip1 regulation of GTPase signaling. *Dev Cell*. 2011;20.
6. Wilson CW, Parker LH, Hall CJ, *et al*. Rasip1 regulates vertebrate vascular endothelial junction stability through Epac1-Rap1 signaling. *Blood*. 2013;122:3678–3690. doi: 10.1182/blood-2013-02-483156.
7. Mitin NY, Ramocki MB, Zullo AJ, Der CJ, Konieczny SF, Taparowsky EJ. Identification and characterization of rain, a novel Ras-interacting protein with a unique subcellular localization. *J Biol Chem*. 2004;279:22353–22361. doi: 10.1074/jbc.M312867200.
8. Mitin N, Konieczny SF, Taparowsky EJ. RAS and the RAIN/RasIP1 effector. *Methods Enzymol*. 2006;407:322–335. doi: 10.1016/S0076-6879(05)07027-8.
9. Post A, Pannekoek WJ, Ponsioen B, Vliem MJ, Bos JL. Rap1 Spatially Controls ArhGAP29 To Inhibit Rho Signaling during Endothelial Barrier Regulation. *Mol Cell Biol*. 2015;35:2495–2502. doi: 10.1128/MCB.01453-14.
10. Vicente-Manzanares M, Ma X, Adelstein RS, Horwitz AR. Non-muscle myosin II takes centre stage in cell adhesion and migration. *Nat Rev Mol Cell Biol*. 2009;10:778–790. doi: 10.1038/nrm2786.
11. de Kreuk BJ, Gingras AR, Knight JD, Liu JJ, Gingras AC, Ginsberg MH. Heart of glass anchors Rasip1 at endothelial cell-cell junctions to support vascular integrity. *Elife*. 2016;5:e11394. doi: 10.7554/eLife.11394.
12. Post A, Pannekoek WJ, Ross SH, Verlaan I, Brouwer PM, Bos JL. Rasip1 mediates Rap1 regulation of Rho in endothelial barrier function through ArhGAP29. *Proc Natl Acad Sci U S A*. 2013;110:11427–11432. doi: 10.1073/pnas.1306595110.
13. Strilić B, Kucera T, Eglinger J, Hughes MR, McNagny KM, Tsukita S, Dejana E, Ferrara N, Lammert E. The molecular basis of vascular lumen formation in the developing mouse aorta. *Dev Cell*. 2009;17:505–515. doi: 10.1016/j.devcel.2009.08.011.
14. Strilić B, Eglinger J, Krieg M, Zeeb M, Axnick J, Babál P, Müller DJ, Lammert E. Electrostatic cell-surface repulsion initiates lumen formation in developing blood vessels. *Curr Biol*. 2010;20:2003–2009. doi: 10.1016/j.cub.2010.09.061.
15. Koo Y, Barry DM, Xu K, Tanigaki K, Davis GE, Mineo C, Cleaver O. Rasip1 is essential to blood vessel stability and angiogenic blood vessel growth. *Angiogenesis*. 2016;19:173–190. doi: 10.1007/s10456-016-9498-5.
16. Dutta D, Williamson CD, Cole NB, Donaldson JG. Pitstop 2 is a potent inhibitor of clathrin-independent endocytosis. *PLoS One*. 2012;7:e45799. doi: 10.1371/journal.pone.0045799.
17. Willox AK, Sahraoui YM, Royle SJ. Non-specificity of Pitstop 2 in clathrin-mediated endocytosis. *Biol Open*. 2014;3:326–331. doi: 10.1242/bio.20147955.
18. Tapon N, Hall A. Rho, Rac and Cdc42 GTPases regulate the organization of the actin cytoskeleton. *Curr Opin Cell Biol*. 1997;9:86–92.
19. Zandvakili I, Davis AK, Hu G, Zheng Y. Loss of RhoA Exacerbates, Rather Than Dampens, Oncogenic K-Ras Induced Lung Adenoma Formation in Mice. *PLoS One*. 2015;10:e0127923. doi: 10.1371/journal.pone.0127923.
20. Yang L, Wang L, Zheng Y. Gene targeting of Cdc42 and Cdc42GAP affirms the critical involvement of Cdc42 in filopodia induction, directed migration, and proliferation in primary mouse embryonic fibroblasts. *Mol Biol Cell*. 2006;17:4675–4685. doi: 10.1091/mbc.E06-05-0466.
21. Zhou X, Florian MC, Arumugam P, Chen X, Cancelas JA, Lang R, Malik P, Geiger H, Zheng Y. RhoA GTPase controls cytokinesis and programmed necrosis of hematopoietic progenitors. *J Exp Med*. 2013;210:2371–2385. doi: 10.1084/jem.20122348.
22. Gu Y, Filippi MD, Cancelas JA, Siefring JE, Williams EP, Jasti AC, Harris CE, Lee AW, Prabhakar R, Atkinson SJ, Kwiatkowski DJ, Williams DA. Hematopoietic cell regulation by Rac1 and Rac2 guanosine triphosphatases. *Science*. 2003;302:445–449. doi: 10.1126/science.1088485.
23. Barry DM, Xu K, Meadows SM, Zheng Y, Norden PR, Davis GE, Cleaver O. Cdc42 is required for cytoskeletal support of endothelial cell adhesion during blood vessel formation in mice. *Development*. 2015;142:3058–3070. doi: 10.1242/dev.125260.
24. Ando K, Fukuhara S, Moriya T, Obara Y, Nakahata N, Mochizuki N. Rap1 potentiates endothelial cell junctions by spatially controlling myosin II activity and actin organization. *J Cell Biol*. 2013;202:901–916. doi: 10.1083/jcb.201301115.
25. Lecuit T, Yap AS. E-cadherin junctions as active mechanical integrators in tissue dynamics. *Nat Cell Biol*. 2015;17:533–539. doi: 10.1038/ncb3136.
26. Bertet C, Sulak L, Lecuit T. Myosin-dependent junction remodelling controls planar cell intercalation and axis elongation. *Nature*. 2004;429:667–671. doi: 10.1038/nature02590.
27. Gebala V, Collins R, Geudens I, Phng LK, Gerhardt H. Blood flow drives lumen formation by inverse membrane blebbing during angiogenesis in vivo. *Nat Cell Biol*. 2016;18:443–450. doi: 10.1038/ncb3320.
28. Denker E, Sehring IM, Dong B, Audisso J, Mathiesen B, Jiang D. Regulation by a TGFβ-ROCK-actomyosin axis secures a non-linear lumen expansion that is essential for tubulogenesis. *Development*. 2015;142:1639–1650. doi: 10.1242/dev.117150.
29. Marty-Santos L, Cleaver O. Pdx1 regulates pancreas tubulogenesis and E-cadherin expression. *Development*. 2016;143:101–112. doi: 10.1242/dev.126755.
30. Totsukawa G, Wu Y, Sasaki Y, Hartshorne DJ, Yamakita Y, Yamashiro S, Matsumura F. Distinct roles of MLCK and ROCK in the regulation of membrane protrusions and focal adhesion dynamics during cell migration of fibroblasts. *J Cell Biol*. 2004;164:427–439. doi: 10.1083/jcb.200306172.
31. Nobes CD, Hall A. Rho, rac, and cdc42 GTPases regulate the assembly of multimolecular focal complexes associated with actin stress fibers, lamellipodia, and filopodia. *Cell*. 1995;81:53–62.

32. Wójciak-Stothard B, Entwistle A, Garg R, Ridley AJ. Regulation of TNF-alpha-induced reorganization of the actin cytoskeleton and cell-cell junctions by Rho, Rac, and Cdc42 in human endothelial cells. *J Cell Physiol*. 1998;176:150–165. doi: 10.1002/(SICI)1097-4652(199807)176:1<150::AID-JCP17>3.0.CO;2-B.
33. Meadows SM, Ratliff LA, Singh MK, Epstein JA, Cleaver O. Resolution of defective dorsal aortae patterning in Sema3E-deficient mice occurs via angiogenic remodeling. *Dev Dyn*. 2013;242:580–590. doi: 10.1002/dvdy.23949.
34. Norden PR, Kim DJ, Barry DM, Cleaver OB, Davis GE. Cdc42 and k-Ras Control Endothelial Tubulogenesis through Apical Membrane and Cytoskeletal Polarization: Novel Stimulatory Roles for GTPase Effectors, the Small GTPases, Rac2 and Rap1b, and Inhibitory Influence of Arhgap31 and Rasa1. *PLoS One*. 2016;11:e0147758. doi: 10.1371/journal.pone.0147758.
35. Villasenor A, Chong DC, Cleaver O. Biphasic Ngn3 expression in the developing pancreas. *Dev Dyn*. 2008;237:3270–3279. doi: 10.1002/dvdy.21740.
36. Xu K, Chong DC, Rankin SA, Zorn AM, Cleaver O. Rasip1 is required for endothelial cell motility, angiogenesis and vessel formation. *Dev Biol*. 2009;329:269–279. doi: 10.1016/j.ydbio.2009.02.033.
37. Koh W, Mahan RD, Davis GE. Cdc42- and Rac1-mediated endothelial lumen formation requires Pak2, Pak4 and Par3, and PKC-dependent signaling. *J Cell Sci*. 2008;121:989–1001. doi: 10.1242/jcs.020693.
38. Jones EA, Baron MH, Fraser SE, Dickinson ME. Dynamic in vivo imaging of mammalian hematovascular development using whole embryo culture. *Methods Mol Med*. 2005;105:381–394.
39. Kalaskar VK, Lauderdale JD. Mouse embryonic development in a serum-free whole embryo culture system. *J Vis Exp*. 2014;85:50803. doi:10.3791/50803.

Novelty and Significance

What Is Known?

- Murine RASIP1 is necessary in endothelial cells for cell adhesion and the formation of continuous vascular lumens.
- RASIP1 is required for the activity of several GTPase-dependent signaling pathways, including Cdc42, Rac1, RhoA, and Rap1.

What New Information Does This Article Contribute?

- Downstream of Rasip1, both Cdc42-Pak and RhoA-ROCK signaling pathways converge on different subcellular pools of NMII to drive lumen formation and regulate vessel diameter, respectively.
- Cdc42-Pak4 signaling mediates actomyosin contractility to remodel endothelial cell adhesions at the preapical membrane between contacting endothelial cells. This allows the formation of a lumen in blood vessels during vasculogenesis.
- Rasip1 suppression of RhoA-ROCK signaling via Arhgap29 acts later to counter myosin-dependent apical membrane contractility/tension, to allow expansion of lumen diameters.

Understanding the mechanisms of blood vessel lumen formation may further anti-angiogenic approaches that aim to block deleterious vascular growth in diseases such as cancer and diabetic retinopathy. Here, we identify Rasip1 as a promising anti-angiogenesis candidate, which is required for the formation of continuous vascular lumens in growing vessels. Further, we elucidate molecular bottlenecks during vessel formation by dissecting the cellular events that require Rasip1. We show that Rasip1 controls different GTPase signaling pathways that converge on the actomyosin contractility machinery. We find that different pools of NMII, downstream of Rasip1, control 2 different processes in endothelial cells: (1) NMII mediates the removal of preapical membrane adhesions to form a lumen. (2) NMII then restrains apical membrane expansion, thereby limiting lumen diameter during vessel growth. In the first process, Rasip1 promotes actin contractility via Cdc42 and Pak4 along ribbons of adhesions at the center of EC cords, causing adhesions to clear from the preapical membrane. This allows opening of lumens. Subsequently, Rasip1 inhibits NMII and membrane contractility via RhoA suppression to allow regulated lumen expansion. These novel and spatiotemporally distinct molecular and cellular events define the step-wise process of blood vessel morphogenesis and differentiation.